SNC Oxygen Fugacity Recorded in Pyroxenes and its Implications for the Oxidation State of the Martian Interior: An Experimental and Analytical Study

M. C. McCanta and M. J. Rutherford' Brown University, Department of Geological Sciences, Box 1846, Providence, RI 02912, molly_mccanta@brown.edu.

Introduction

Knowledge of the oxidation state of a magma is critical as it is one of the parameters which controls the nature and composition of the resulting crystals [Eugster, 1957; Eugster and Wones, 1962; Carmichael, 1967; Frost and Lindsley, 1991]. In terrestrial magmatic systems, oxygen fugacity (f_{O2}) is known to vary by over nine orders of magnitude [Carmichael, 1991; Parkinson and Arculus, 1999]. With variations of this magnitude, understanding the compositional differences, phase changes, and crystallization sequence variations, caused by the magma f_{O2}, is essential in deciphering the origin of all igneous rocks.

Magmatic oxidation state is of great importance in that it reflects the degree of oxidation of the source region and can provide insight into magmatic processes, such as metasomatism, degassing, and assimilation, which may have changed them. Carmichael [1991] argues that most magmas are unlikely to have their redox states altered from those of their source region. This assumption allows for estimation of the oxidation state of planetary interiors. Conversely, it is known that the f_{O2} of the magma can be affected by other processes, which occur outside of the source region and therefore, the oxidation state may record those too. Processes which could overprint source region fugacities include melt dehydrogenation or other volatile loss, water or melt infiltration, or assimilation of oxidized or reduced wallrock [Brandon and Draper, 1996; Ague, 1998; Frost and Ballhaus, 1998; Parkinson and Arculus, 1999]. Understanding which of these processes is responsible for the redox state of a magma can provide crucial information regarding igneous processes and other forces active in the region.

The composition of the SNC basalts and their widely varying proposed oxidation states raise some interesting questions. Do the SNC meteorites have an oxidized or reduced signature? What was the oxygen fugacity of the SNC source region at the time of melt generation? Is the fugacity calculated for the various SNC samples the fugacity of the magma source region or was it overprinted by later events? Are there different oxidation states in the Martian interior or a single one? This proposal seeks to address all of these questions.

Progress Report

Task 1a of the original proposal has been completed. All present publications resulting from this are presented in the references. This task consisted of an assessment of the variation of Eu-valence state in early crystallized, experimental low-Ca pyroxenes (pigeonite, Pgt) with magmatic f_{O2}, with an emphasis on constraint of the oxidation state recorded in the basaltic shergottites. Fugacity was measured in the pyroxenes using two techniques which utilize oxidation state proxies of $D(Eu/Gd)_{pgt/melt}$ and $D(Eu/Sm)_{pgt/melt}$. The results of this task provide a new way to measure Martian f_{O2}.

Task 1. SNC f_{O_2} recorded in pyroxenes: An experimental study.

Experiments to characterize pyroxene composition have been conducted over a range of representative magmatic f_{O2}'s. Dry crystallization experiments were performed on a starting composition composed of a synthetic shergottite melt in equilibrium with liquidus pyroxenes, A^*_M (see Johnson *et al.* [1991]). The melt was doped with ~1wt.% each of Eu_2O_3, Gd_2O_3, and Sm_2O_3 following the method of McKay *et al.* [1986]. Experiments were run at the Johnson Space Center in one-atmosphere, CO-CO_2 gas mixing furnaces using Re-loops. The dry experiments were run over a range of representative magmatic f_{O2}s, from highly reduced IW-2 to moderately oxidized IW+3.5 (equivalent to QFM, quartz-fayalite-magnetite). The f_{O2} was controlled through the mixing of the CO and CO_2 gases, and measured with an external ZrO_2 sensor. All dry runs were held at 1235°C for 30 minutes to ensure melt homogenization. Runs were then cooled to 1165°C, 15-20°C below the dry liquidus temperature determined by Minitti and Rutherford [2000] for a similar starting composition, at 60°C/hour. Charges were held for 24 hours to facilitate crystal nucleation and growth. Samples were then rapidly quenched and the products thin sectioned.

Hydrous crystallization experiments were also performed on A^*_M in TZM (tungsten-zirconium-molybdenum) pressure vessels at Brown University. Experiments were run at 1110°C and $P_{total}=P_{H2O}=200$ bars. Experimental f_{O2}'s ranged from oxidizing, nickel-nickel oxide (NNO = IW+4.5), to reducing, graphite-methane (IW+0.5). The higher f_{O2} runs were buffered using pre-determined mixtures of Ar and CH_4 gases appropriate for the desired f_{O2}. These runs included powdered buffer assemblages in separate tubes within the experimental capsules to monitor the f_{O2}. For example, $Ni_{(m)}$ and NiO were placed inside all NNO runs. At the end of the run the presence of both phases was verified. Runs which contained only one phase were discarded. The low f_{O2} experiment was buffered through the breakdown of CH_4 gas. To better approximate the liquidus, runs were initially pressurized to 500 bars and held for 24 hours. Runs were then slowly decompressed over ~2 hours to a final pressure of 200 bars, corresponding to approximately 1.5 wt.% water, an amount determined to be plausible for SNC magmas by Minitti and Rutherford [2000]. This pressure drop initiated pyroxene crystallization. Runs were held for at least 24 hours to facilitate crystal nucleation and growth. Samples were then rapidly quenched and the products thin sectioned.

All experimental phenocryst phases and melts were analyzed for their major element compositions on the Brown University Cameca Camebax and SX-100 electron microprobes. Eu/Gd and Eu/Sm ratios in the pyroxenes and coexisting melt were measured on the Woods Hole Oceanographic Institution Cameca 3F and Arizona State University Cameca 6F ion microprobes.

The results of both the dry and hydrous experiments are given in Figure 1 [McCanta and Rutherford, 2001; McCanta et al., 2002a]. For a dry basaltic shergottite melt, the average $D(Eu/Gd)_{pyx/melt}$ range from 0.156(f_{O2}=IW-1) to 0.639(QFM). $D(Eu/Sm)_{pyx/melt}$ range from 0.279(IW-1) to 1.135(QFM). The $D(Gd/Sm)_{pyx/melt}$ is 1.76±0.02, indicating all variation in Figure 1 is due to Eu variation. This new Eu-oxybarometer calibration for pigeonite yields refined f_{O2} values for the basaltic shergottites, ranging from IW+3.1 for Shergotty to IW+0.2 for QUE94201. These numbers differ in value, but not trend, from those published previously [e.g. Herd et al., 2001; Wadhwa, 2001]. These f_{O2} values were calculated using natural pigeonite core data from Wadhwa et al. [1994]. The f_{O2}'s calculated from our pigeonites [McCanta et al., 2002b; McCanta and Rutherford, 2002] are similar to those determined in a recent calibration of augite REE distribution coefficients vs. f_{O2} [Musselwhite and Jones, 2002; Musselwhite and Wadhwa, 2002] and to those determined using recent Fe-Ti oxide data [Herd et al., 2000] (Figure 2A and B).

For a hydrous basaltic shergottite melt the average $D(Eu/Gd)_{pyx/melt}$ range from 0.62 (f_{O2}=IW+0.5) to 0.69 (IW+4.5). $D(Eu/Sm)_{pyx/melt}$ was not measured in hydrous runs as the starting material was only doped with Gd_2O_3 and Eu_2O_3. The higher f_{O2} results determined in the dry experiments correspond well with results from the hydrous experiments.

Our experimental data provides a calibration of the effects of f_{O2} on pigeonite REE partitioning in both dry and hydrous basaltic shergottite melts. Because pigeonite is one of the first phases to crystallize, this technique allows for the measurement of f_{O2} during the earliest crystallization history of the melt. Both distribution coefficients (Eu/Gd and Eu/Sm) record comparable f_{O2} values for measured Martian meteorites indicating that either method can be used in future analyses.

Our data suggests that the Martian meteorites crystallized under a variety of different f_{O2} conditions. This has been recognized previously in studies of augite [e.g. Wadhwa, 2001]. Our new results from the pigeonite Eu-oxybarometer detailed above show ~2-3 orders of magnitude difference in f_{O2} between the basaltic shergottite meteorites, not as large a range as previously argued. This variation is less than the observed terrestrial variation of ~9 orders of magnitude [e.g. Carmichael, 1991], but much greater than that seen on the moon. Several possibilities exist that could explain the range in Martian f_{O2}. It could reflect intrinsic f_{O2} differences in the magma source regions on Mars (i.e. the Martian mantle or lithosphere), or it could result from interactions between the magma and an assimilant, that is as yet unsampled, either at depth or near the surface. This new f_{O2} data may provide insight into which of these is the more likely explanation.

Experimental studies have shown that pigeonite is one of the first minerals to crystallize from a shergottite melt, whereas Fe-Ti oxides come on the liquidus late in the crystallization sequence (after 30 and 60% crystallization in hydrous and dry experiments, respectively, to possibly 95% in Los Angeles) [e.g. Minitti and Rutherford, 2000; Xirouchakis et al., 2002]. Therefore, pigeonite core f_{O2} values should record a different portion of magmatic history than the oxides. However, when the pigeonite f_{O2} values are compared with the most recent determination of Fe-Ti oxide f_{O2} values, a close correlation is observed (Figure 2B). This implies that the melt f_{O2} for each of these meteorites was buffered internally throughout much of the crystallization sequence. That is, the early crystallizing minerals were exposed to the same relative f_{O2} environment as the late crystallizing minerals. These results are consistent with the argument that the variations in f_{O2} recorded in the basaltic shergottites are the result of intrinsic f_{O2} differences in the magma source regions of these rocks. However, assimilation cannot be completely ruled out on this basis alone. If the assimilation occurred before any crystallization had taken place, the primary f_{O_2} recorded in the phenocrysts would be that of the source region modified by the assimilant.

Task 1b: Investigation of Henry's Law behavior of REE in pigeonite.

Several tasks were originally proposed to help illuminate the oxidation state of the Martian interior. The first task, discussed in the progress report above, has been completed as stipulated in the original proposal. An additional question arose as a result of the data collected in Task 1a relating to the Henry's Law behavior of the REEs which were doped to weight percent levels in the experiments. In order to address this question, new experiments were completed on starting compositions containing 0.5 and 0.1 weight percent REE, respectively, as opposed to the original starting composition doped with 1.0 weight percent REEs. These runs were run in the gas mixing furnaces at Johnson Space Center over the same range of f_{O_2} conditions as the original experiments. All run products were analyzed for their REE concentrations on the Arizona State University Cameca 6F ion microprobe. The data collected was compared to the data presented above and it was determined that Henry's Law had not been violated in any of the Eu-oxybarometer calibration experiments (Figure 3). This task provided confidence in the pigeonite Eu-oxybarometer and the Martian crystallization f_{O_2} values the pigeonite record.

References

Ague J.J. (1998) Simple models of coupled fluid infiltration and redox reactions in the crust. *Contrib. Mineral. Petrol.* **132**, 180-197.

Bogard D.D. and Johnson P. (1983) Martian gases in an Antarctic meteorite. *Science* **221**, 651-654.

Brandon A.D. and Draper D.S. (1996) Constraints on the origin of the oxidation state of mantle overlying subduction zones: an example from Simcoe, Washington, USA. *Geochim. Cosmochim. Acta* **60**, 1739-1749.

Carmichael I.S.E. (1991) The oxidation state of basic magmas: a reflection of their source region? *Contrib. Mineral. Petrol.* **106**, 129-142.

Delaney J.S., Sutton S.R., and Dyar M.D. (1998) Variable oxidation states of iron in Martian meteorites (abstr.). *Lunar Planet. Sci.* **29**, 1241-1242, CD-ROM.

Eugster H.P. (1957) Heterogeneous reactions involving oxidation and reduction at high pressures and temperatures. *J. Chem. Phys.* **26**, 1760.

Eugster H.P. and Wones D.R. (1962) Stability relations of the ferruginous biotite, annite. *J. Petrol.* **3**, 82-125.

Frost B.R. and Lindsley D.H. (1991) Occurrence of iron-titanium oxides in igneous rocks. In Lindsley, Donald, ed. Oxide Minerals, *Rev. Mineral.*, **v.25**. Mineral. Soc. Am., Washington, D.C., 433-468.

Frost B.R. and Ballhaus C. (1998) Comment on "Constraints on the origin of the oxidation state of mantle overlying subduction zones: an example from Simcoe, Washington, USA". *Geochim. Cosmochim. Acta* **62**, 329-331.

Ghosal S., Sack R.O., Ghiorso M.S., and Lipschutz M.E. (1998) Evidence for a reduced, Fe-depleted Martian mantle source region of shergottites. *Contrib. Mineral. Petrol.* **130**, 346-357.

Hale V.P.S., McSween H.Y., Jr., and McKay G.A. (1999) Re-evaluation of intercumulus liquid composition and oxidation state for the Shergotty meteorite. *Geochim. Cosmochim. Acta* **63**, 1459-1470.

Herd C.D.K. and Papike J.J. (1998) Estimates of oxygen fugacity in the basaltic shergottites from electron microprobe oxygen analysis (abstr.). *Geo. Soc. Am. Abstr. Prog.* **31**, 44-45.

Herd C.D.K. and Papike J.J. (1999) Implications for the petrogenesis of Martian meteorite Dar al Gani 476 from spinel, olivine, and pyroxene compositions (abstr.). *Geo. Soc. Am. Abstr. Prog.* **30**, 288.

Herd C.D.K. and Papike J.J. (2000) Oxygen fugacity of the Martian basalts from analysis of iron-titanium oxides: implications for mantle-crust interactions on Mars (abstr.). *Met. Plan. Sci.* **34**.

Johnson M.C., Rutherford M.J., and Hess P.C. (1991) Chassigny petrogenesis: melt inclusions, intensive parameters, and water content of martian magmas. *Geochim. Cosmochim. Acta* **55**, 349-366.

McCanta M.C. and Rutherford M.J. (2001) SNC oxygen fugacity as recorded in pyroxenes: an experimental study (abstr.). *Lunar Planet. Sci.* **32**.

McCanta M.C., Rutherford M.J., and Jones J.H. (2002a) An experimental study of Eu/Gd partitioning between a shergottite melt and pigeonite: implications for the oxygen fugacity of the Martian interior (abstr.). *Lunar Planet. Sci.* **33**.

McCanta M.C., Rutherford M.J., and Musselwhite D.S. (2002b) An experimental study of REE partitioning between a dry shergottite melt and pigeonite as a function of f_{O_2}; implications for the martian interior (abstr.). *Met. Planet. Sci.* **37**, A97.

McCanta M.C. and Rutherford M.J. (2002) Oxygen fugacity recorded in pigeonite: indications of a heterogeneous martian magma source region? (abstr.). Unmixing the SNCs workshop, 6013.

McKay G., Wagstaff J., and Yang S.-R. (1986) Clinopyroxene REE distribution coefficients for shergottites: the REE content of the Shergotty melt. *Geochim. Cosmchim. Acta* **50**, 927-937.

McKay G., Le L., Wagstaff J., and Crozaz G. (1994) Experimental partitioning of rare earth elements and strontium: constraints on petrogenesis and redox conditions during crystallization of Antarctic angrite Lewis Cliff 86010. *Geochim. Cosmochim. Acta* **58**, 2911-2919.

McSween H.Y., Jr. (1985) SNC meteorites: clues to Martian petrologic evolution? *Rev. Geophys.* **23**, 391-416.

McSween H.Y., Jr. (1994) What we have learned about Mars from SNC meteorites. *Meteoritics* **29**, 757-779.

Minitti M.E. and Rutherford M.J. (2000) Genesis of the Mars Pathfinder "sulfur-free" rock from SNC parental liquids. *Geochim. Cosmochim. Acta* **64**, 2535-2547.

Musselwhite D.S. and Jones J.H. (2002) Variation in the augite/melt partitioning of Sm, Eu, and Gd with fO2: implications for the oxidation state of the martian mantle (abstr.). *Met. Planet. Sci.* **37**, A106.

Musselwhite D.S. and Wadhwa M. (2002) REE in shergottite augites and whole rocks (abstr.). Unmixing the SNCs workshop, 6024.

Parkinson I.J. and Arculus R.J. (1999) The redox state of subduction zones: insights from arc peridotites. *Chem. Geol.* **160**, 409-423.

Sato M., Hickling N.L., and McLane J.E. (1973) Oxygen fugacity values of Apollo 12, 14, and 15 lunar samples and reduced state of lunar magmas. *Proc. Lunar Sci. Conf.* **4**, 1061-1079.

Wadhwa M. (2000) Quantitative constraints on the redox state of Martian magmas from Eu anomalies in pyroxenes of basaltic shergottites (abstr). *Lunar Planet. Sci.* **31**, 1966, CD-ROM.

Wadhwa M. (2001) Redox state of Mars' upper mantle and crust from Eu anomalies in shergottite pyroxenes.*Science,* **291**, 1527-1530.

Figure Captions

Figure 1. Dry and hydrous calibration of $D(Eu/Gd)_{pigeonite}$ versus f_{O2} (in log units relative to the IW buffer). Error bars on the distribution coefficients indicate the standard deviation between ion microprobe analyses of the materials in the same sample. Solid line is the best-fit curve (2nd order polynomial) for each system.

Figure 2. (A) Comparison with augite Eu-oxybarometer calibration of Musselwhite and Jones (2002) using shergottitic melt starting composition. S: Shergotty, EA: EETA79001 lithology A, EB: EETA79001 lithology B, Z: Zagami, Q: QUE94201. Pigeonite f_{O2} error bars are 2σ. Augite f_{O2} error from Musselwhite and Jones (2002). (B) Comparison of f_{O2} calculated using dry pigeonite Eu-oxybarometer versus Fe-Ti oxide equilibria (Herd *et al.*, 2001). Solid line is a 1:1 line. Pigeonite f_{O2} error bars are 2σ. Oxide f_{O2} error from Herd *et al.* (2001).

Figure 3. Dry calibration of $D(Eu/Gd)_{pigeonite/melt}$ and $D(Eu/Sm)_{pigeonite/melt}$ versus f_{O2} (in log units relative to the IW buffer) for 1.0 wt.% REE experiments. Pgt: pigeonite. Solid line is the best-fit curve (2nd order polynomial) for each system. Squares are measured data for Henry's Law experiments with 0.1 wt.% of REEs. Note that the low-REE runs plot either on top of or within error of the high-REE runs. For example, at f_{O2} = IW+3.5, the two $D(Eu/Gd)_{pigeonite/melt}$ data points are identical, while the two $D(Eu/Sm)_{pigeonite/melt}$ data points are the same within error. Error bars on the distribution coefficients indicate the standard deviation between ion microprobe analyses of the materials in the same sample.

Publications

McCanta M.C., Rutherford M.J., and Jones J.H. (in publication) An experimental study of rare earth element partitioning between a shergottite melt and pigeonite: implications for the oxygen fugacity of the martian interior. *Geochim. Cosmochim. Acta.*

McCanta M.C., Rutherford M.J., Dyar M.D., and Delaney J.S. (2003) $Fe^{3+}/\Sigma Fe$ ratios in pigeonite as a function of f_{O2}: a preliminary investigation (abstr.). *Lunar Planet. Sci.* **34**.

McCanta M.C. and Rutherford M.J. (2002) Oxygen fugacity recorded in pigeonite: indications of a heterogeneous martian magma source region? (abstr.). Unmixing the SNCs workshop, 6013.

McCanta M.C., Rutherford M.J., and Jones J.H. (2002a) An experimental study of Eu/Gd partitioning between a shergottite melt and pigeonite: implications for the oxygen fugacity of the martian interior (abstr.). *Lunar Planet. Sci.* **33**.

McCanta M.C., Rutherford M.J., and Musselwhite D.S. (2002b) An experimental study of REE partitioning between a dry shergottite melt and pigeonite as a function of f_{O2}; implications for the martian interior (abstr.). *Met. Planet. Sci.* **37**, A97.

McCanta M.C. and Rutherford M.J. (2001) SNC oxygen fugacity as recorded in pyroxenes: an experimental study (abstr.). *Lunar Planet. Sci.* **32**.

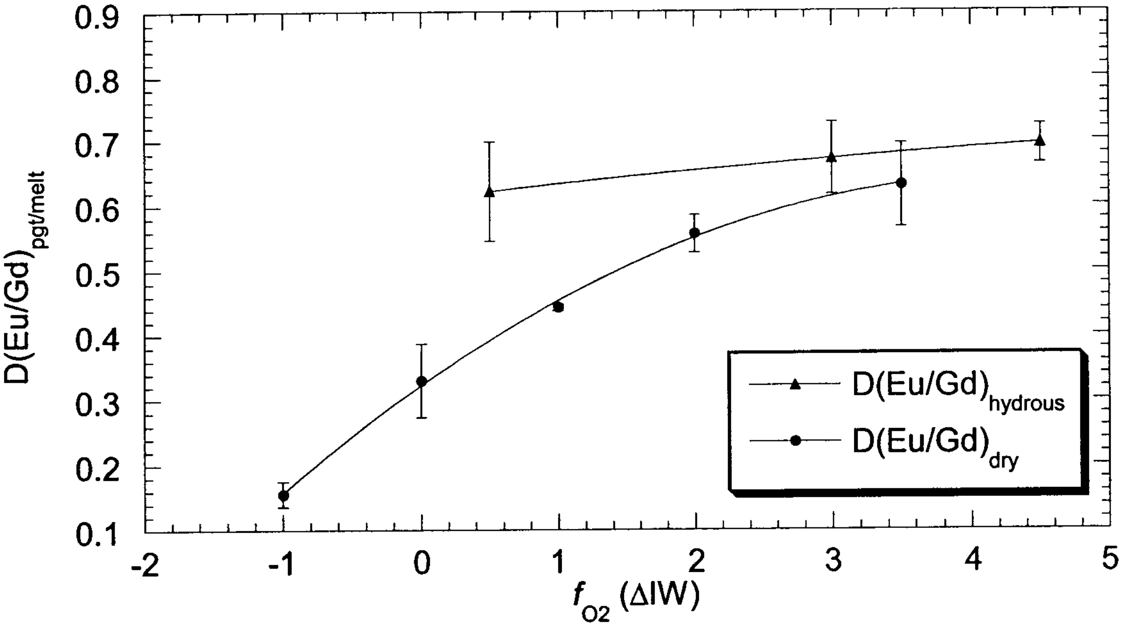
0.9
0.8
0.7
0.6
0.5
0.4
0.3
0.2
0.1
$D(Eu/Gd)_{pgt/melt}$
-2
-1
0
1
2
3
4
5
f_{O2} (ΔIW)
$D(Eu/Gd)_{hydrous}$
$D(Eu/Gd)_{dry}$

Figure 1.

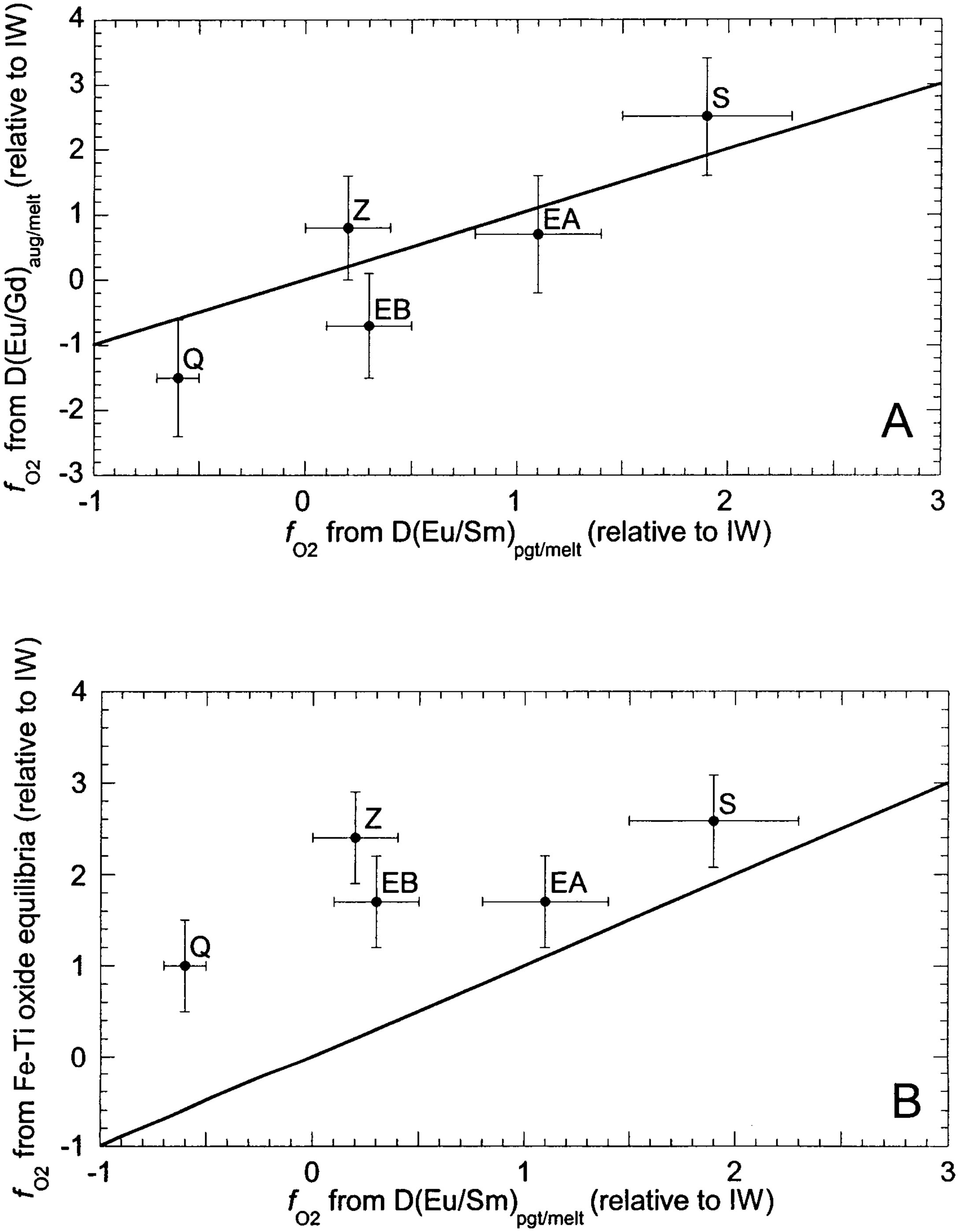

4
3
2
1
0
-1
-2
-3
f_{O2} from D(Eu/Gd)$_{aug/melt}$ (relative to IW)
S
Z
EA
EB
Q
A
-1
0
1
2
3
f_{O2} from D(Eu/Sm)$_{pgt/melt}$ (relative to IW)
4
3
2
1
0
-1
f_{O2} from Fe-Ti oxide equilibria (relative to IW)
S
Z
EB
EA
Q
B
-1
0
1
2
3
f_{O2} from D(Eu/Sm)$_{pgt/melt}$ (relative to IW)

Figure 2.

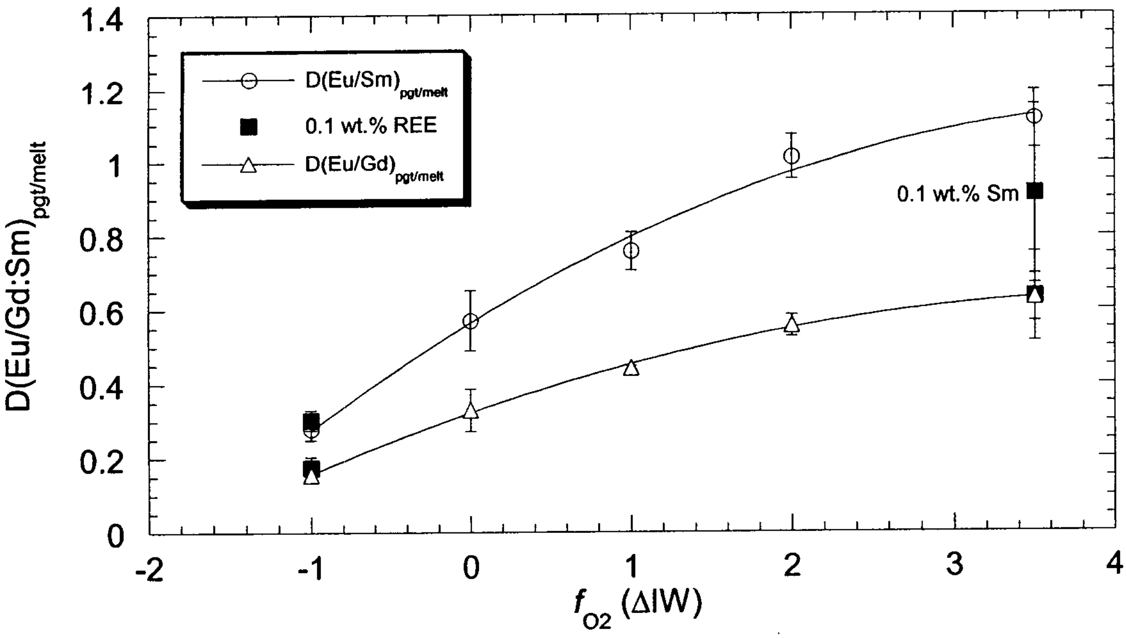

D(Eu/Sm)pgt/melt
0.1 wt.% REE
D(Eu/Gd)pgt/melt
0.1 wt.% Sm
D(Eu/Gd:Sm)pgt/melt
1.4
1.2
1
0.8
0.6
0.4
0.2
0
-2
-1
0
1
2
3
4
fO2 (ΔIW)

Figure 3.